Robust damping controller design for a static compensator

A.H.M.A. Rahim, S.A. Al-Baiyat and H.M. Al-Maghrabi

Abstract: A robust controller for providing damping to power system transients through static compensator (STATCOM) devices is presented. The method of multiplicative uncertainty has been employed to model the variations of the operating points in the system. A loop-shaping method has been employed to select a suitable open-loop transfer function, from which the robust controller is constructed. The design is carried out applying robustness criteria for stability and performance. The proposed controller has been tested through a number of disturbances including three-phase faults. The robust controller designed has been demonstrated to provide extremely good damping characteristics over a range of operating conditions.

1 Introduction

It is well established that reactive compensation of transmission lines through rapidly variable solid state thyristor switches of FACTS devices improves both the transient and the dynamic performance of a power system [1]. These devices dynamically control the power flow through a variable reactive admittance to the transmission network. Controllable synchronous voltage sources, known as static compensators, are a recent introduction in power systems for dynamic compensation and for real-time control of power flow. The static compensator (STATCOM) provides shunt compensation in a similar way to the static VAr compensator (SVC) but utilizes a voltage source converter rather than shunt capacitors and reactors [2]. The basic principle of operation of a STATCOM is the generation of a controllable AC voltage source behind a transformer leakage reactance by a voltage source converter connected to a DC capacitor. The voltage difference across the reactance produces active and reactive power exchanges between the STATCOM and the power system [3].

Two basic controls are implemented in a STATCOM. The first is the AC voltage regulation of the power system, which is realised by controlling the reactive power interchange between the STATCOM and the power system. The other is the control of the DC voltage across the capacitor through which the active power injection from the STATCOM to the power system is controlled [3, 4]. The effect of stabilising controls on STATCOM controllers has been investigated also in several recent reports [4, 5]. PI controllers have been found to provide stabilising controls when the AC and DC regulators were designed independently. However, joint operations of the two have been reported to lead to system instability because of the interaction of the two controllers [3, 5]. While superimposing the damping controller on the AC regulator can circumvent the negative interaction problem, the fixed parameter PI controllers have been found invalid, or even to provide negative damping for certain system parameters and loading conditions [6]. Application of controls that performed over a range of operating conditions has also been reported in recent times. Farasangi [7] proposed a robust controller for SVC and STATCOM devices using H_∞ techniques. Robust control for FACTS devices and their interaction with loads were examined by Ammari [8]. These designs are often complicated, restricting their realisation.

This paper presents a simple technique for designing a robust damping controller for a power system installed with a STATCOM. The variations of the operating conditions in the power system have been taken into consideration by modelling them as multiplicative unstructured uncertainty. A loop-shaping technique [9] has been employed to design the controllers. It was observed that a robust controller in the speed loop, with nominal voltage feedback, effectively damps the electromechanical oscillations for a wide range of operating conditions.

2 Power system model

A single machine infinite bus system with a STATCOM connected through a step-down transformer is shown in Fig. 1. The robust controller is designed considering a low-order dynamic model of the generator to give the 'worst-case' scenario. The assumptions made are [6]:

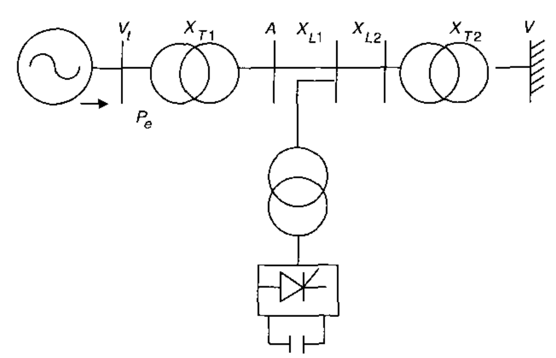

Fig. 1 *Single machine system with STATCOM*

IEE Proceedings online no. 20020344

DOI: 10.1049/ip-gtd:20020344

Paper first received 14th March 2001 and in revised form 28th November 2001

The authors are with the Department of Electrical Engineering, K.F. University of Petroleum and Minerals, Dhahran 31261, Saudi Arabia

a. No detailed exciter and governor dynamic models; constant generator voltage e_q' behind reactance x_d'; damping is neglected; mechanical power input P_m is constant.

b. STATCOM is a reactive current source with time delay. Inductive current generated by STATCOM is assumed positive.

The system is described by the following equations:

$$\begin{aligned} \Delta\dot{\delta} &= \omega_o \Delta\omega \\ \Delta\dot{\omega} &= \frac{1}{2H}[D\Delta\omega - \Delta P_e] \\ \Delta\dot{I}_S &= \frac{K}{T}[-\Delta I_S + C\Delta u] \end{aligned} \quad (1)$$

Here δ, ω, $2H$, D represent the load (torque) angle, angular speed, inertia constant and damping constant, respectively. The delivered electrical power P_e is expressed as

$$P_e = \frac{e_q' V_m}{x_d' + x_1}\sin\theta + \frac{V_m^2}{2}\frac{x_d' - x_q}{(x_d' + x_1)(x_q + x_1)}\sin 2\theta \quad (2)$$

The direct and quadrature axis components of mid-bus voltage V_m are written as

$$V_{mq} = \frac{(x_1 + x_d')V_o\cos\delta + e_q' x_2 + I_S x_2(x_1 + x_d')\cos\theta}{x_1 + x_2 + x_d'} \quad (3)$$

$$V_{md} = \frac{(x_1 + x_q)V_o\sin\delta + I_S x_2(x_1 + x_q)\sin\theta}{x_1 + x_2 + x_q} \quad (4)$$

θ is the phase difference between the quadrature axis of the generator and V_m, and is given by $\tan\theta = V_{md}/V_{mq}$.

By linearising (2)–(4), the STATCOM controller input is written as

$$\Delta u = -C_v \Delta V_m + C_\omega \Delta\omega \quad (5)$$

The linearised system block diagram is shown in Fig. 2.

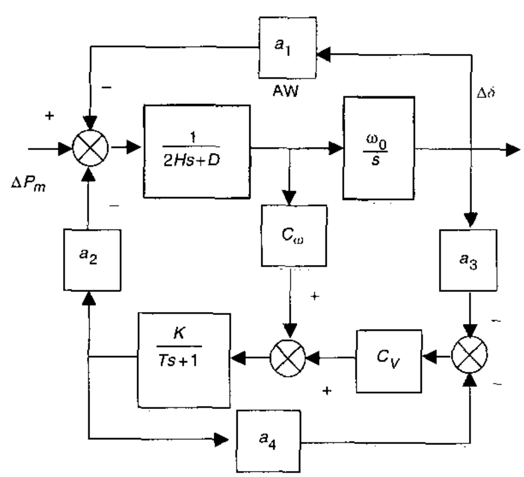

Fig. 2 *Block diagram of the linearised system*

3 Robust control design

The damping control problem for the nonlinear power system model is stated as: given the nonlinear set of (1)–(4), find control u that will stabilize the system following a perturbation. Since there is no general method of optimising the design for the nonlinear system, one way would be to perform the control design for a linearised system, the linearisation being carried out around a nominal operating condition. If the controller designed is 'robust' enough to perform well for the other operating points in the vicinity, the design objectives are met.

The changes in operating points of the nonlinear system can be considered as changes in the coefficients $a_1 \ldots a_4$ of the linearised model given in Fig. 2. These perturbations are modelled as multiplicative uncertainties and robust design procedure is applied to the perturbed linear systems. This section gives a brief theory of the uncertainty model, the robust stability criterion, and a graphical design technique termed loop shaping, which is employed to design the robust controller. Finally, the algorithm for the control design is presented.

3.1 Uncertainty modelling

Suppose that a plant having a nominal transfer function P belongs to a bounded set of transfer functions **P**. Consider that the perturbed transfer function resulting from the variations in operating conditions can be expressed in the form

$$\tilde{P} = (1 + \Omega W_2)P \quad (6)$$

Here, W_2 is a fixed stable transfer function, also called the weight, and Ω is a variable transfer function satisfying $||\Omega||_\infty < 1$. The infinity norm (∞-norm) of a function is the least upper bound of its absolute value, also written as $||\Omega||_\infty = \sup_\omega|\Omega(j\omega)|$, and is the largest value of gain on a Bode magnitude plot.

In the multiplicative uncertainty model (6), ΩW_2 is the normalised plant perturbation away from 1. If $||\Omega||_\infty < 1$, then

$$\left|\frac{\tilde{P}(j\omega)}{P(j\omega)} - 1\right| \le |W_2(j\omega)|, \forall\omega \quad (7)$$

$|W_2(j\omega)|$ provides the uncertainty profile, and in the frequency plane is the upper boundary of all the normalised plant transfer functions away from 1.

3.2 Robust stability and performance

Consider a multi-input control system given in Fig. 3. A controller C provides stability if it provides internal stability for every plant in the uncertainty set **P**. If L denotes the open-loop transfer function ($L = PC$), then the sensitivity function S is written as

$$S = \frac{1}{1 + L} \quad (8)$$

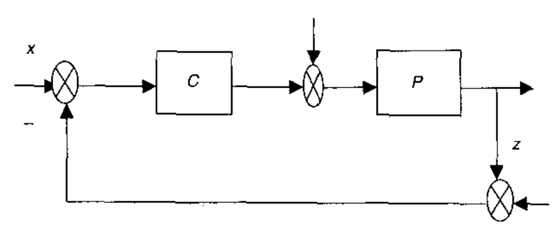

Fig. 3 *Controller configuration*

For a multiplicative perturbation model, the robust stability condition is met if and only if $||W_2 T||_\infty < 1$ [9, 10]. This implies that

$$\left|\frac{W_2(j\omega)L(j\omega)}{1 + L(j\omega)}\right| < 1, \text{ for all } \omega \quad (9)$$

T is the complement of S, and is the input–output transfer function.

The block diagram of a typical perturbed system, ignoring all inputs, is shown in Fig. 4*a*. The transfer function from the output of Ω to the input of Ω is $-W_2T$. The properties of the block diagram can be reduced to those of the configuration given in Fig. 4*b*.

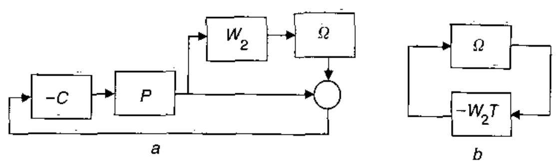

Fig. 4 *Perturbed feedback system with controller and the reduced block diagram*

The maximum loop gain, $\|-W_2T\|_\infty$, is less than 1 for all allowable Ω, if and only if the small gain condition $\|W_2T\|_\infty < 1$ holds. The nominal performance condition for an internally stable system is given as $\|W_1S\|_\infty < 1$, where W_1 is a real, rational, stable, minimum phase transfer function, also called a weighting function [9].

The robust performance condition is

$$\|W_2T\|_\infty < 1 \text{ and } \left\|\frac{W_1S}{1+\Omega W_2T}\right\| < 1,\ \forall\|\Omega\| < 1 \tag{10}$$

Combining all the above, it can be shown that a necessary and sufficient condition for robust performance is [9]

$$\||W_1S| + |W_2T|\|_\infty < 1 \tag{11}$$

3.3 Loop-shaping technique

Loop shaping is a graphical procedure to design a proper controller C satisfying robust stability and performance criteria given above. The basic idea of the method is to construct the loop transfer function L to satisfy the robust performance criterion approximately, and then to obtain the controller from the relationship $C = L/P$. Internal stability of the plants and properness of C constitute the constraints of the method. The condition on L is such that PC should not have any pole zero cancellation.

A necessary condition for robustness is that either or both $|W_1|, |W_2|$ must be less than 1 [10]. If we select a monotonically decreasing W_1 satisfying the other constraints on it, it can be shown that at low frequency the open-loop transfer function L should satisfy

$$|L| > \frac{|W_1|}{1-|W_2|} \tag{12}$$

while, for high frequency,

$$|L| < \frac{1-|W_1|}{|W_2|} \approx \frac{1}{|W_2|} \tag{13}$$

At high frequency $|L|$ should roll-off at least as quickly as $|P|$ does. This ensures properness of C. The general features of the open-loop transfer function are that the gain at low frequency should be large enough, and $|L|$ should not drop off too quickly near the crossover frequency resulting in internal instability.

3.4 Algorithm

The algorithm to generate a control transfer function C so that robust stability and robust performance conditions are met involves the following steps:

1. Obtain the dB-magnitude plot for the nominal as well as perturbed plant transfer functions.
2. Construct W_2 satisfying (7).
3. Select W_1 as a monotonically decreasing, real, rational and stable function.
4. Choose L such that it satisfies (12) and (13). The transition at crossover frequency should not be at a slope steeper than −20 dB/decade. Nominal internal stability is achieved if, on a Nyquist plot of L, the angle of L at crossover is greater than 180°.
5. Check for the nominal and robust performance criteria given in Section 3.2.
6. Test for internal stability by direct simulation of the closed-loop transfer function for pre-selected disturbance or input.
7. Repeat steps 4 to 6 until satisfactory L and C are obtained.

4 Implementation

As shown in Fig. 2, there are two control functions C_ω and C_v in the speed and voltage loops of the STATCOM voltage regulator, respectively. The effect of the robust controller in these loops was examined independently, followed by their coordinated application. The data for the generator–STATCOM system are included in the Appendix (Section 8).

4.1 Robust speed controller design

In the absence of the voltage loop in the STATCOM control system, only parameters a_1 and a_2 in Fig. 2 appear in the system model. For generator output of 0.8 pu at unity power factor, the collapsed system of Fig. 3 gives the following nominal plant function:

$$P_{nom} = \frac{1.0435s}{(s+50)(s^2+60.66)} \tag{14}$$

Here, controller C is replaced by C_ω. Off-nominal power outputs in the range 0.2–1.2 pu and power factors 0.8 lagging to 0.8 leading were considered. The dB against frequency plot for the nominal and perturbed plants is shown in Fig. 5. The quantity $|\tilde{P}(j\omega)/P(j\omega) - 1|$ is constructed for each perturbed plant and the maximum magnitude is fitted to the function

$$W_2(s) = \frac{0.8s^2 + 2.24s + 39.2}{s^2 + 0.98s + 49} \tag{15}$$

A Butterworth filter satisfies all the properties for $W_1(s)$ and is written as

$$W_1(s) = \frac{Kf_c^2}{s^3 + 2s^2f_c + 2sf_c^2 + f_c^3} \tag{16}$$

For these W_1 and W_2, and for open-loop transfer function

$$L(s) = \frac{208.75(s+1)(s+2)}{(s+0.01)(s+50)(s^2+60.66)} \tag{17}$$

the controller transfer function from the relation $C_\omega = L/P$ is

$$C_\omega(s) = \frac{200(s+1)(s+2)}{s(s+0.01)} \tag{18}$$

The dB magnitude plot relating W_1, W_2 and L, which was employed to arrive at the controller, is shown in Fig. 6. The plots for the nominal performance and robust performance measures are shown in Fig. 7.

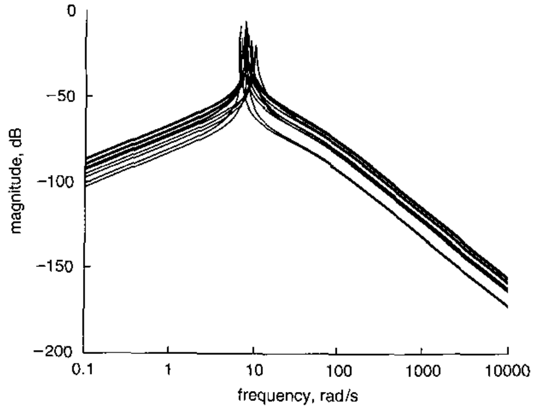

Fig. 5 *Bode diagram for the nominal and perturbed plant transfer functions*

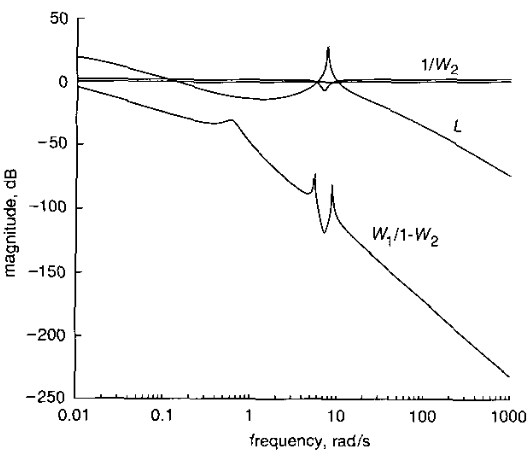

Fig. 6 *Plots of W_1, W_2 and L for loop-shaping*

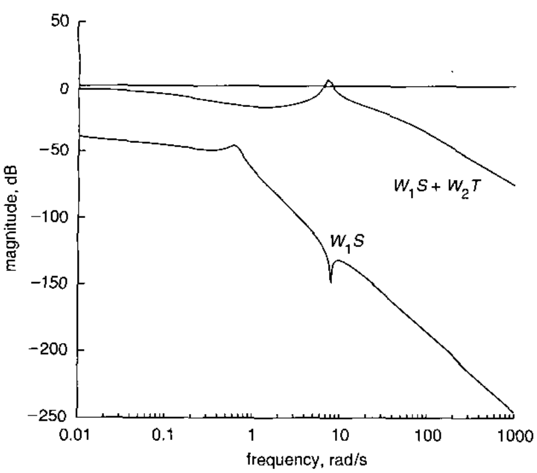

Fig. 7 *Plot of robust and nominal performance indices*

The robust STATCOM speed controller was tested by applying a 100% input torque pulse to the generator for 0.05 s duration. The generator torque angle variations for a number of operating conditions, including that for the nominal plant, are plotted in Fig. 8. It can be observed that good damping properties can be obtained with the robust

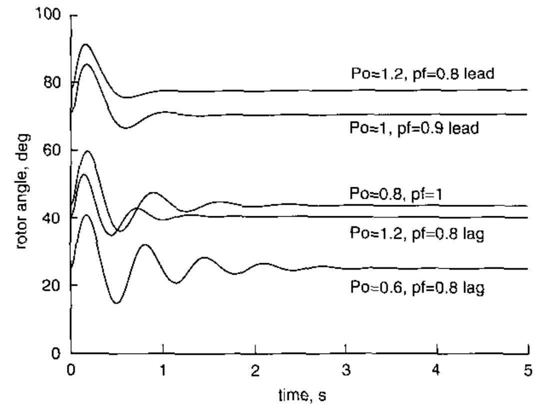

Fig. 8 *Torque angle-time characteristics with the robust speed-controller for different loading conditions*

speed controller over a wide range of operating conditions. The controller can be designed to provide more damping, but the steady state error and the overshoot in the bus voltages may be excessive in such cases. Note that PI controllers reported in the literature do not provide adequate damping, and additionally require retuning for varying operating conditions.

4.2 Robust controller design in the voltage loop

Repeating the procedure of Section 4.1 with the controller in the voltage loop alone, the nominal plant transfer function for the particular operating condition is expressed as

$$P_{nom} = \frac{-10.31885(s^2 + 65.505)}{(s + 50)(s^2 + 60.7316)} \tag{19}$$

The nominal plant is in a positive feedback loop and may be internally stable only for a limited range of operation, so does not satisfy the general conditions of robust design. If C_v takes the opposite sign, stability can be imposed over a broader range.

Following similar steps to those taken in Section 4.1, the controller function for this P_{nom} is obtained as

$$C_v(s) = \frac{(s + 1)(s + 50)(s^2 + 60.73)}{(s + 0.01)(s^2 + 65.5)(s^2 + s + 60.73)} \tag{20}$$

The rotor angle characteristics of the generator and mid-bus voltage variations for a range of operating conditions are shown in Figs. 9 and 10, respectively. The robust design does provide adequate damping particularly at the operating conditions near the nominal ones, but they are not as good as those with the damping controller in the speed loop. Note that earlier studies indicate that a STATCOM voltage control loop does not provide good damping to the system [4, 11]. PI controller designs are often unsatisfactory and may even lead to unstable situations [11].

4.3 Coordinated robust speed and voltage controllers

The robust controllers designed independently in the speed and voltage loops were applied simultaneously. The response obtained for the nominal as the well as the perturbed plant for simulated disturbances showed very good transient control over a wide range of operating conditions. The initial onslaught of the transients was quickly eliminated, but very low-level oscillations were observed to continue. Although the C_v controller does not provide enough damping, it has been observed to have an

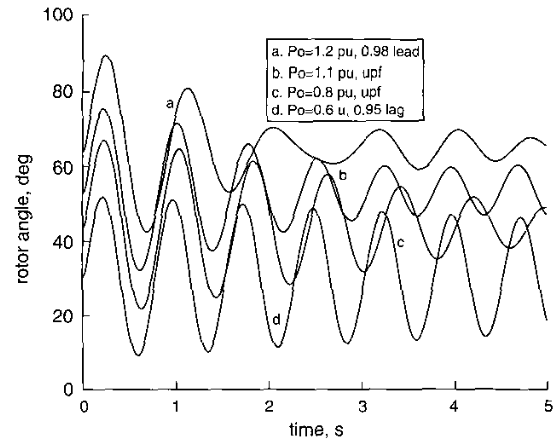

Fig. 9 *Torque angle-time characteristics with the robust voltage-controller for different loading conditions*

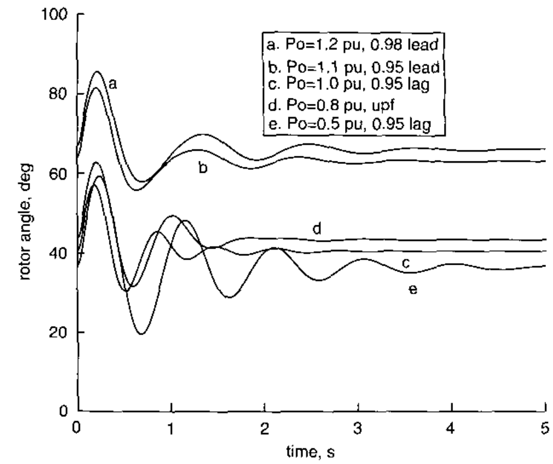

Fig. 11 *Generator torque angle variations with the coordinated robust speed-voltage-controller for various loading conditions*

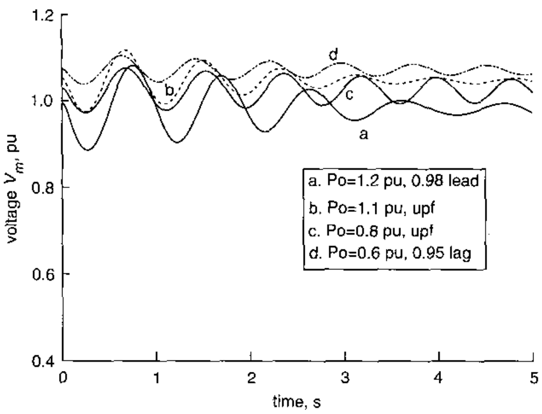

Fig. 10 *Mid-bus voltage variations with the robust voltage-controller corresponding to Fig. 9*

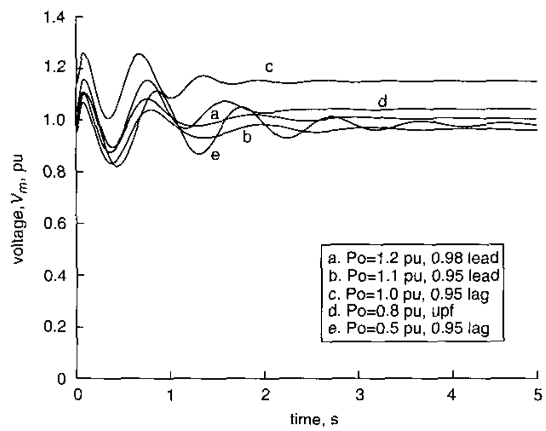

Fig. 12 *Mid-bus voltage variations corresponding to Fig. 11 for various loading conditions*

important role in voltage regulation. In order to give C_ω a larger role in damping control, the robust controller was redesigned by setting C_v to a nominal value of 1 and repeating the procedure so that robust stability and performance conditions are met. The nominal plant transfer in this case is

$$P(s) = \frac{1.043s^2}{(s + 58.6249)(s^2 + 1.694s + 10.69)} \tag{21}$$

Satisfying the criteria of the loop-shaping method, the following controller function was arrived at:

$$C(s) = \frac{100(s + 7)(s^2 + 2s + 1)(s^2 + 1.694s + 10.69)}{s^2(s + 0.01)(s^2 + 5s + 49)} \tag{22}$$

The torque angle and the mid-bus voltage variations for five widely varying loading conditions are given in Figs. 11 and 12. As can be observed, the robust controller provides extremely good damping characteristics in all these cases.

4.4 Fault studies

The coordinated robust controller designed through linear system modelling was then applied to the nonlinear power system model. In the nonlinear model, (2)–(4) have to be solved at each integration step iteratively. For a three-phase

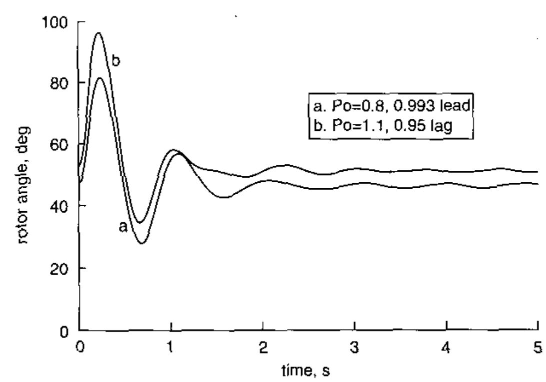

Fig. 13 *Generator torque angle variations with the coordinated controller following a three-phase fault on the remote bus*

fault of 0.1 s duration on the remote bus, the generator torque angle and the bus voltage are shown in Figs. 13 and 14, respectively, using the coordinated robust speed-voltage controller. In the fault studies, responses for only two loading conditions have been shown. These are: (a) nominal power output of 0.8 pu at almost unity power factor, and (b) pre-fault generator output of 1.1 pu at 0.95 lagging

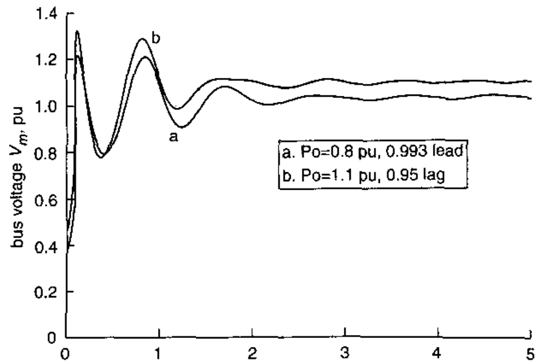

Fig. 14 *Mid-bus voltage characteristics corresponding to Fig. 13 following a three-phase fault on the remote bus*

power factor. The pre-fault voltage profile is almost flat over the entire transmission line in the first case. The transient profile with a fault on the overloaded machine shows the control design is extremely robust.

5 Conclusions

A method of designing a robust damping controller for a STATCOM has been proposed. The design was carried out employing both robust stability and robust performance considerations. The controller was tested for a number of disturbance conditions including symmetrical three-phase faults. The robust design has been found to be very effective for a range of operating conditions of the power system. The operating conditions for which the controller provides good performance depend on the spectrum of perturbed plants selected in the design process. The robust design is much superior to conventional PI and other similar controllers, where the controller coefficients normally need to be retuned for various operating conditions. The graphical loop-shaping method utilised to determine the controller function is simple and straightforward to implement.

6 Acknowledgment

The authors wish to acknowledge the facilities provided at the King Fahd University of Petroleum and Minerals, Dhahran, Saudi Arabia.

7 References

1 GYUGYI, L.: 'Dynamic Compensation of AC Transmission Lines by Solid-State Synchronous Voltage Sources', *IEEE Trans. Power Deliv.*, 1994, **9**, (2), pp. 904–911
2 MACHOWSKI, J.: 'Power System Dynamics and stability', (John Wiley and Sons, 1997)
3 WANG, H., and LI, F.: 'Multivariable Sampled Regulators for the Co-ordinated Control of STATCOM AC and DC Voltage', *IEE Proc., Gener., Transm. Distrib.*, 2000, **147**, (2), pp. 93–98
4 WANG, H.F., and LI, F.: 'Design of STATCOM Multivariable Sampled Regulator'. Int. Conf. on Electric Utility Deregulation and Power Tech. 2000, City University, London, April 2000
5 WANG, H.F.: 'Phillips-Heffron Model of Power Systems Installed with STATCOM and Applications', *IEE Proc., Gener., Transm. Distrib.*, 1999, **146**, (5), pp. 521–527
6 LI, C., JIANG, O., WANG, Z., and RETZMANN, D.: 'Design of a Rule Based Controller for STATCOM'. Proc. 24th Annual Conf. of IEEE Ind. Electronic Society, IECon '98, 1998, Vol. 1, pp. 467–472
7 FARASANGI, M.M., SONG, Y.H., and SUN, Y.Z.: 'Supplementary Control Design of SVC and STATCOM Using H_∞ Optimal Robust Control'. Proc. Int. Conf. on Electric Utility Deregulation 2000, City University, London, April 2000, pp. 355–360
8 AMMARI, S., BESANGER, Y., HADJSAID, N., and GEORGES, D.: 'Robust Solutions for the Interaction Phenomena between Dynamic Loads and FACTS Controllers'. Proc. IEEE PES Summer Meeting 2000, Vol. 1, pp. 401–406
9 DOYLE, J.C., FRANCIS, B.A., and TANNENBAUM, A.R.: 'Feedback Control Theory' (MacMillan Publishing Co., New York, 1992)
10 LEVINE, W.S.: 'The Control Handbook', (CRC Press and IEEE Press, 1996)
11 PADIYAR, K.R., and DEVI, A.L.: 'Control and Simulation of Static Condenser', *APEC 94-9th Annual Applied Power Electronics Conference and Exposition*, 1994, 1, (2), pp. 826–831

8 Appendix

The system parameters (in per unit) are: $X_d' = 0.22$, $x_d = 1.96$, $x_q = 0.4$ $D = 0$ $H = 3.35\,\text{s}$ $x_{T1} = x_{T2} = 0.1$ $x_{L1} = 0.2$ $x_{L2} = 0.3$ $T = 0.02\,\text{s}$ $K = 1$